Article

Heating Performance and Energy Efficiency Analysis of Air-Source Heat Pumps in Public Buildings Across Different Climate Zonings

Junbao Fan [1], Yilin Liu [1,*], Jing Ma [2], Ying Cao [1,2], Zhibin Zhang [1], Xin Cui [1] and Liwen Jin [1,*]

[1] School of Human Settlements and Civil Engineering, Xi'an Jiaotong University, No. 28 Xianning West Road, Xi'an 710049, China
[2] China Architecture Design and Research Group, Beijing 100044, China
* Correspondence: ylliu@xjtu.edu.cn (Y.L.); lwjin@xjtu.edu.cn (L.J.)
Received: 11 July 2024; Revised: 3 September 2024; Accepted: 5 September 2024; Published: 20 September 2024

Abstract: Public buildings exhibit the highest operational energy consumption and contribute the most to carbon emissions compared to other types of building. The electrification of energy terminals in public buildings is crucial for the energy conservation and emission reduction, especially the energy-saving retrofitting of heating systems. Given the significant impact of climate on the performance of air-source heat pumps, this study explored the performance and energy efficiency of air-source heat pump systems in public buildings across different climate zonings. Using Design Builder software, the physical models of three types of public buildings (commercial, hotel, and office) were constructed, and the annual variations in the building load was analyzed. Considering the effects of defrosting and low-temperature conditions, an air-source heat pump heating system models were developed using TRNSYS software. The simulation results showed that the average COP of the heat pump system on the coldest day in Harbin, Beijing, and Shanghai were 1.7, 2.46 and 2.49, respectively. Moreover, the analysis factor correlation analysis reveals that the COP of the heat pump system is positively correlated with the dry-bulb temperature, negatively correlated with the building load. Surprisingly, the COP is not affected by the types of public buildings. The findings of this study are expected to provide valuable guidance for the application and regulation of air-source heat pumps in the public buildings.

Keywords: air-source heat pump; public building; heating; coefficient of performance; correlation analysis

1. Introduction

As of 2021, public buildings had the highest operational energy consumption intensity among all building types. Although the total area of public buildings is only 14.7 billion square meters, much smaller than that of urban and rural residential buildings, public buildings account for the largest proportion of total operational energy consumption in China, approximately 34.7%, amounting to 386 million tons of standard coal equivalent. Correspondingly, the carbon emissions from the operation of public buildings also constitute the highest proportion of total building operational carbon emissions, approximately 32.7%, reaching 720 million tons of CO_2 [1]. Accelerating the adjustment of the energy structure, increasing the proportion of clean energy, promoting electrification, and reducing the dependence on fossil fuels are effective ways to achieve the "dual carbon" goals [2]. The electrification of building energy terminals is a key measure to reach these goals, especially in enhancing the electrification level of the heating in public buildings.

In recent years, air-source heat pumps, as an efficient and energy-saving clean heating technology, have effectively utilized low-grade energy from the ambient air, thereby conserving the higher-grade energy sources [3–6]. They are currently widely used in regions with hot-summers and cold-winters in China, such as the Yangtze River Basin and its southern areas [7]. In the northeastern and northwestern regions, the growth and potential for air-source heat pumps are substantial due to coal policy restrictions and increasing coal prices [8]. Researchers have conducted extensive studies on the factors affecting the performance of air-source heat pumps and their application strategies [9,10].

The air-source heat pump is prone to frosting at low ambient temperatures, which can significantly impair its operating performance. Integrating the air-source heat pump with other energy systems or optimizing the circulating system can effectively enhance system performance. Xu et al. [11] investigated the impact of climate

conditions on the frost formation in air-source heat pumps and proposed a characterization parameter, namely the hours of the frost formation. By analyzing the hours of the frost formation under various characteristic temperature differences and combining the frost characteristics of different types of air-source heat pumps, the climate division for China was conducted to provide a reference for the climate-adaptive design and defrost control strategies for air-source heat pumps. Wu et al. [12] experimentally tested the long-term performance of an air-source heat pump system under cold climate conditions. The experimental data showed that the system coefficient of performance (COP) is highly correlated with the outdoor temperature. When the supply water temperature increased by approximately 6 °C and the outdoor temperature was around -5 °C, the corresponding COP decreased by 14.2%. Additionally, the relative humidity had a minimal impact on the system COP. Wu et al. [13] constructed a heating system combining an air-source heat pump with a water storage tank and conducted a long-term performance monitoring in an actual building in Beijing. The coupled system allowed the air-source heat pump to operate continuously at higher ambient temperatures. The results revealed that, compared to the continuous operation, the daily average COP of the air-source heat pump increased by 14.0% and the SCOP increased by 26.1% on the coldest days. Long et al. [14] proposed a hybrid combined heating system integrating the solar hot water with an air-source heat pump, and analyzed its energy efficiency during the cold season. The results indicated that the solar radiation intensity and the ambient temperature were the crucial factors affecting the energy efficiency of various connection methods within the combined system. Changes in the return water temperature had the greatest impact on the series configuration and the least impact on the parallel configuration. By switching the connection method between solar heat water (SHW) and air-source heat pump (ASHP) based on outdoor weather conditions, the HSAHP combined with the heating system can achieve significant energy-saving benefits.

In general, the research on the air-source heat pump mainly focuses on its design optimization, environmental applications, and integration with other heating methods, primarily in residential buildings [15–20]. There is a lack of research concerning its use in the heating system of public buildings. The application of ASHP in public buildings significantly differs from the residential settings in terms of building load magnitude, hourly load variation, and system operation times. Additionally, the ASHP is commonly used as single units in residential buildings, whereas large public buildings typically require simultaneous use of multiple units. Moreover, importantly, in low-temperature environments, the performance of ASHP may decline significantly due to frost formation. Furthermore, the performance of air-source heat pump systems exhibits significant variations under different building types and climate zonings. Therefore, it is imperative to explore the suitability and actual performance trends of ASHPs in different public building types across different climate zonings in China.

In this study, to explore the effects of building types and climate zonings on the performance of air-source heat pumps, the representative cities (Harbin, Beijing, and Shanghai) were selected for severe cold, cold, and hot-summer and cold-winter regions, respectively. The physical models of three typical types of public buildings (commercial, hotel, and office) were constructed using Design Builder software to analyze the annual variations in the building load. Considering the effects of defrosting and low-temperature conditions, the air-source heat pump heating system models were developed using TRNSYS software. By utilizing annual hourly load data from three types of public buildings in the three representative cities, the operational characteristics and performance influencing factors of air-source heat pump systems on the typical days (hottest day, moderate-temperature day, and coldest day) were simulated and analyzed. The findings of this study are expected to provide effective guidance for the application and control strategies of air-source heat pump systems in public buildings.

2. Model Development of Air Source Heat Pump System

2.1. Selection of Typical Cities

There is a vast territory with significant climate differences across various regions in China, which can be classified into five climate zones: severe cold, cold, hot-summer and cold-winter, hot summer and warm winter, and mild regions. The air-source heat pump is primarily used for the heating in low-temperature areas, with the heating performance greatly influenced by outdoor climate parameters. Therefore, this study focuses on the severe cold, cold, and hot-summer and cold-winter zones. The climatic features of severely cold regions are predominantly characterized by extremely cold and prolonged winters, significant annual and daily temperature variations, with the temperature in winter frequently dropping below −10 °C. In cold regions, the climate is characterized by cold and dry winters, accompanied by large annual and daily temperature differences. The temperature in winter typically ranges from −10 °C to 0 °C, with a considerable number of days where the daily average temperature is lower than 5 °C. On the other hand, the climatic features of hot-summer and cold-winter regions are more intricate, featuring sultry and humid summers and chilly and dry winters. The temperature in summer often exceeds 30 °C, while the temperature in winter may dip to around 0 °C. The comprehensive

investigation identifies the representative cities for these three climate zones as Harbin, Beijing, and Shanghai, respectively. The heating durations for these three cities are shown in Table 1.

Given the diverse types of public buildings, this study selects three typical categories as the research subjects: commercial, hotel, and office buildings. Referring to the actual building information provided by China Architecture Design and Research Group, the physical model of typical public buildings: commercial, hotels, and office buildings were built based on the Design Builder software, as shown in Figure 1. The office building has a floor-to-ceiling height of 7 stories, a total building height of 30.6 m, and a total floor area of 9280 square meters. The primary room functions include office spaces and meeting rooms. The hotel building comprises a 3-story low-rise section and a 15-story high-rise section, with a total building height of 52.5 m and a total floor area of 34,000 square meters. The main room functions encompass dining, lodging, and various other facilities. The commercial building has a floor-to-ceiling height of 4 stories, a total building height of 23 m, and a total floor area of 135,000 square meters. The key functions include retail, dining, supermarkets, and cinemas. The annual hourly heat load variations for three Harbin, Beijing, and Shanghai public buildings were simulated and analyzed. The resulting load data served as the input parameters for the operation simulation of air-source heat pump system.

Table 1. The heating durations for three typical cities.

Climate Zonings	City	Heating Condition	Heating Duration
Severe cold	Harbin	$T_{ave} \leq 5$ ℃	10.17~04.10
Cold	Beijing	$T_{ave} \leq 5$ ℃	11.12~03.14
Hot-summer and cold-winter	Shanghai	$T_{ave} \leq 8$ ℃	12.05~03.07

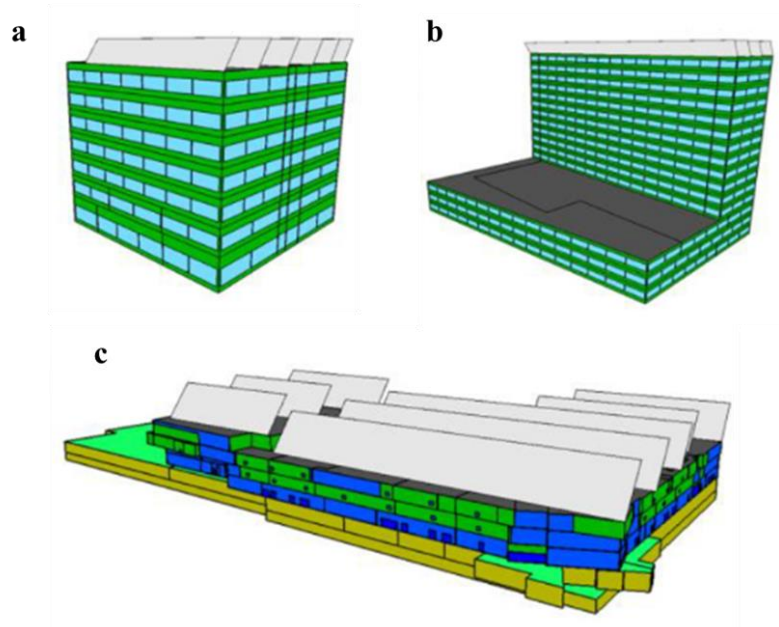

Figure 1. The model diagrams constructed using design builder: (**a**) Office building; (**b**) Hotel building; (**c**) Commercial building.

2.2. Air-Source Heat Pump System Model

The TRNSYS software can perform the transient energy consumption simulations for systems, featuring high visualization capabilities and good openness, which is widely used in multi-zone building models and HVAC systems [21]. As shown in Figure 2, the air-source heat pump heating system model is constructed based on the TRNSYS software. The system comprises an air-source heat pump circuit (red loop) and a terminal heating circuit (purple loop). The red loop section comprises an air-source heat pump module, a buffer tank, a heat pump-side circulating pump, and a heat pump quantity control module. Specifically, the buffer tank collects the heat output from the air-source heat pump module for the terminal heating. Through a comprehensive feedback mechanism, the control module adjusts the number of operating heat pumps based on the hourly heat load, the stored heat in the buffer tank, and the output heat of air-source heat pump. By contrast, the purple loop section includes a buffer tank, supply and return piping, a terminal heating module, and a load-side circulating pump. The buffer tank is

controlled by adjusting the water pump speed to provide the heat to the terminal heating module, thereby satisfying the real-time building load. Additionally, switching the two blue lines completes the switching of the cooling and heating cycles.

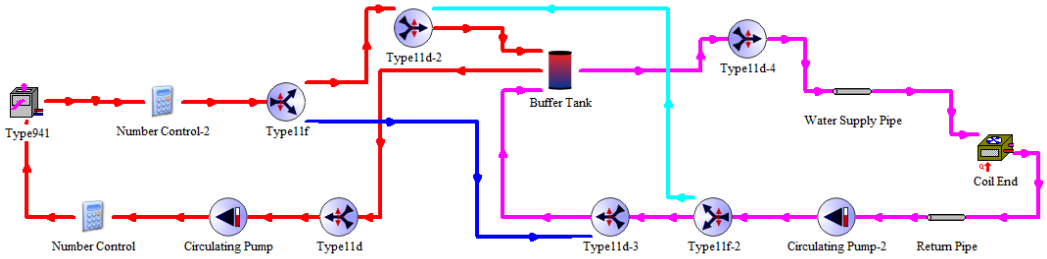

Figure 2. The air-source heat pump heating system.

The air-source heat pump heating system model is established using TRNSYS software, which utilizes various standard components to form a complete loop and generate data output. In the simulation and analysis of heating system, the specific modules are invoked to record data. The simulations are conducted under given input conditions, and the numerical results are collected through the output module. The main standard components involved in the air-source heat pump heating system model used in this study are listed in Table 2.

Table 2. Standard components selected in the TRNSYS model for this study.

Type	Component Name	Type	Component Description
Type941	Air-source Heat Pump	Type165	Controller
Type158	Thermal Storage Tan	Type515	Seasonal Schedule
Type673	Energy Rate Control Load	Type14h	Time Forcing Function
Type11f	Diverter/Mixer Valve	Type9e	General Data File Reader
Type110	Circulation Pump	Type15-3	Energy Climate File
Type31	Circulation Pump	Type65c	Online Plotter
Type24	Integrator	Type46a	Output

2.3. Correction Method for Low Temperature and Defrosting of Air-Source Heat Pumps

To analyze the variable condition performance of air-source heat pumps, this study utilizes performance fitting equations that account for the effects of low temperatures and defrosting to reflect the decay in the heating capacity and input power of air-source heat pump. To analyze the performance of air source heat pump under variable operating conditions, the performance fitting equation considering the effect of low temperature and defrosting on heat pump heating capacity attenuation is adopted in this paper.

(a) Heating capacity correction of the air-source heat pump for low-temperature

The heating capacity of the air-source heat pump on variable operating conditions is positively correlated with the outdoor temperature and negatively correlated with the outlet water temperature of the condenser. The correction coefficient equation for the heating capacity on variable operating conditions is as follows [22].

$$K_1 = a_1 + a_2 t_a + a_3 t_{out,a} + a_4 t_a^{\ 2} + a_5 t_a t_{out,a} + a_6 t_{out,a}^{\ 2} \quad (1)$$

where K_1 denotes the correction coefficient of heat produced by heat pump under low-temperature condition; $a_{1\sim}a_6$ represents the fitting coefficients; t_a denotes the outdoor temperature, °C; $t_{out,a}$ denotes the condenser outlet water temperature, °C.

(b) Heating capacity correction of the air-source heat pump for defrosting

Defrosting in the air-source heat pumps generally involves a reverse heating cycle, which reduces the heating capacity of the heat pump. When the temperature is below 7 °C and above 7 °C, the correction factors for the heating capacity during the defrosting are as follows [7].

$$t_a < 7\ °C,\ \ K_2 = 1 + 0.0027(t_a - 7) - 0.1801\exp(-t_a^{\ 2}/5) \quad (2)$$

$$t_a > 7\ °C,\ \ K_2 = 1 - 0.1801\exp(-t_a^{\ 2}/5) \quad (3)$$

where K_2 is the correction coefficient of heat produced by heat pump under defrosting condition.

(c) Input power correction of the air-source heat pump for low-temperature

The input power of the air-source heat pump on the variable operating conditions is influenced by both the outdoor temperature and the outlet water temperature of the condenser. Therefore, the fitted equation for the input power of the air-source heat pump on variable operating conditions is as follows.

$$K_3 = b_1 + b_2 t_a + b_3 t_{out,a} + b_4 t_a^2 + b_5 t_a t_{out,a} + b_6 t_{out,a}^2 \quad (4)$$

where K_3 represents the correction coefficient for the variable operating condition input power of the air-source heat pump; b_1~b_6 represent the fitting coefficient.

2.4. Performance Characterization Parameters of Air-Source Heat Pump

To evaluate the performance of air-source heat pumps under different setting parameters, three performance indicators are introduced: daily average load, daily average COP, and maximum load. The daily average load ($Q_{H\text{-}ave}$) is calculated with Equation (5), expressed as the arithmetic mean of heat loads during all working hours of the day. The daily average *COP* (COP_{ave}) is determined by Equation (6), which represents the arithmetic mean of the *COP* during all working hours of the day when the heat pump is operating normally. The maximum load occurs at the time point with the maximum absolute value of load during the calculation day.

$$Q_{H-ave} = \sum_{h=1}^{24} Q_H \quad (5)$$

$$COP_{ave} = \sum_{h=1}^{24} COP_h \quad (6)$$

where $Q_{H\text{-}ave}$ is the daily average load, and Q_H is the hourly heat load. COP_{ave} is the average coefficient of performance, and *COP* is the hourly coefficient of performance.

2.5. Selection of Air-Source Heat Pumps

Considering the building load magnitudes in severe cold, cold, and hot-summer and cold-winter zones, the variable frequency air-source heat pump with the heating capacity of 165 kW from Midea is selected. Its performance and design parameters are listed in Tables 3 and 4. Based on the data provided by the manufacturer regarding the outlet water temperature, heat output, and input power of the heat pump under different outdoor ambient temperatures, the aforementioned performance fitting equations are employed to fit the actual performance data. The fitting results yield the heat output correction coefficient K_1 and input power coefficient K_3 of the heat pump under different outdoor ambient temperatures and outlet water temperatures. The correction coefficients for low temperature and defrosting are calculated using Equations (1–4), which are listed in Table 5.

Table 3. The performance parameters of air-source heat pump.

Operation Modes	Parameters	Unit	Value
Nominal heating mode	Nominal heating capacity	kW	110
	Nominal Heating power	kW	41.98
	Water flow rate	m^3/h	18.90
	COP		2.62
Nominal cooling mode	Nominal cooling capacity	kW	142
	Nominal cooling power	kW	41.89
	Water flow rate	m^3/h	24.42
	COP		3.39
Low-temperature heating mode	Low-temperature heating capacity	kW	90
	Low-temperature heating power	kW	50.1
	Water flow rate	m^3/h	18.6
	COP		1.8
Rated heating mode	Rated heating capacity	kW	165
	Rated heating power	kW	44.35
	Water flow rate	m^3/h	28.5
	COP		3.72

Table 4. Design parameters for supply/return water temperature of air-source heat pump heating system in different climate zones.

Climate Zones	Sever Cold	Cold	Hot-Summer and Cold-Winter
Supply/return water temperature	38/33 °C	41/36 °C	45/40 °C

Table 5. Correction and Fitting Coefficients for Variable Operating Condition Heating Capacity and Input Power.

Coefficients	K_1(×10^{-4})	Coefficients	K_3 (×10^{-4})
a_1	7001.3	b_1	7938.6
a_2	133.2	b_2	−13.3
a_3	89.8	b_3	−142.5
a_4	−1.45	b_4	−0.22
a_5	0.36	b_5	0.73
a_6	−1.25	b_6	4.96

3. Dynamic Operating Characteristics of Air-Source Heat Pump Systems

3.1. Distribution Characteristics of Annual Hourly Dynamic Heat Load

To compare and analyze the hourly heat load distribution patterns throughout the year for three regions, Figure 3 presents the annual load and outdoor dry-bulb temperature variation curves for commercial buildings in Harbin, Beijing, and Shanghai. Clearly, the building load is closely correlated with outdoor dry-bulb temperatures, exhibiting different trends across the three regions. In Harbin and Beijing, with lower outdoor temperatures, the building heat load reaches the peak during the middle of heating duration. In contrast, the building load in Shanghai shows a more moderate variation throughout the year. Regarding the heat load data, the building load in Harbin are significantly higher than those in Beijing and Shanghai. The maximum heat load for commercial buildings is 9335.78 kW, with an annual average heat load of 1465.06 kW.

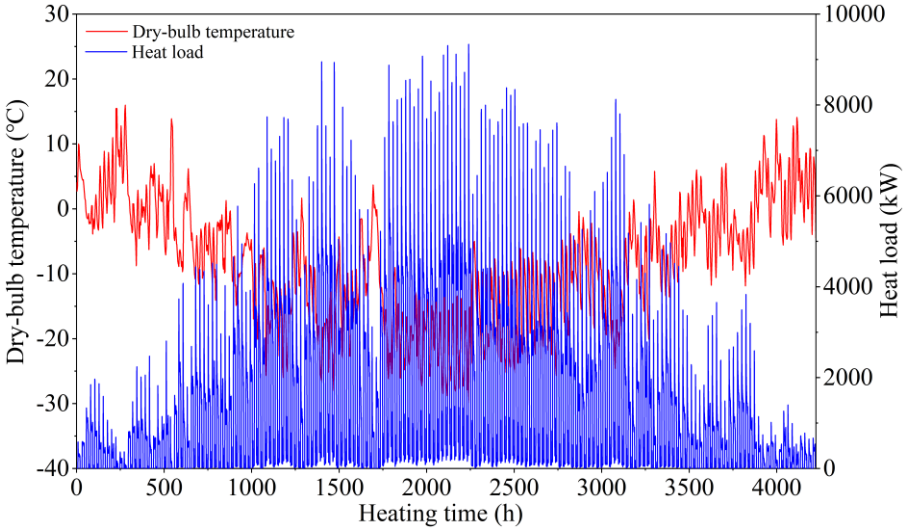

(**a**)

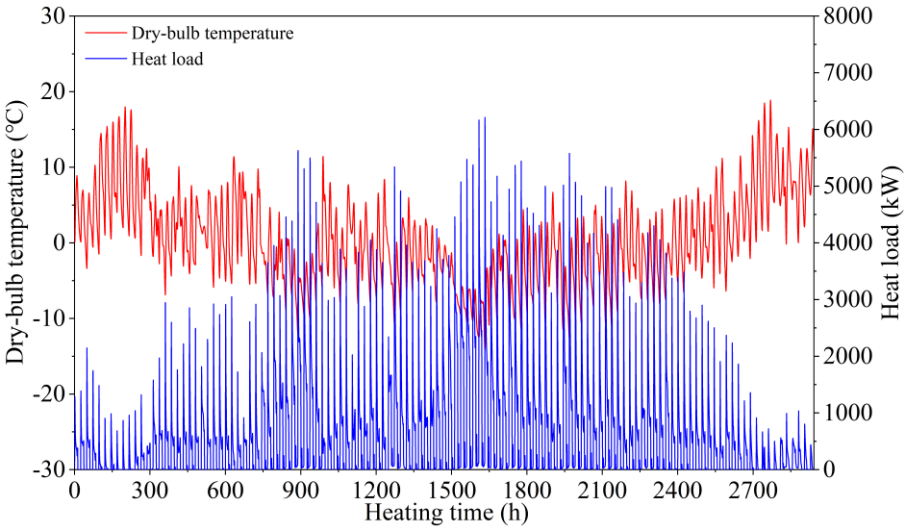

(**b**)

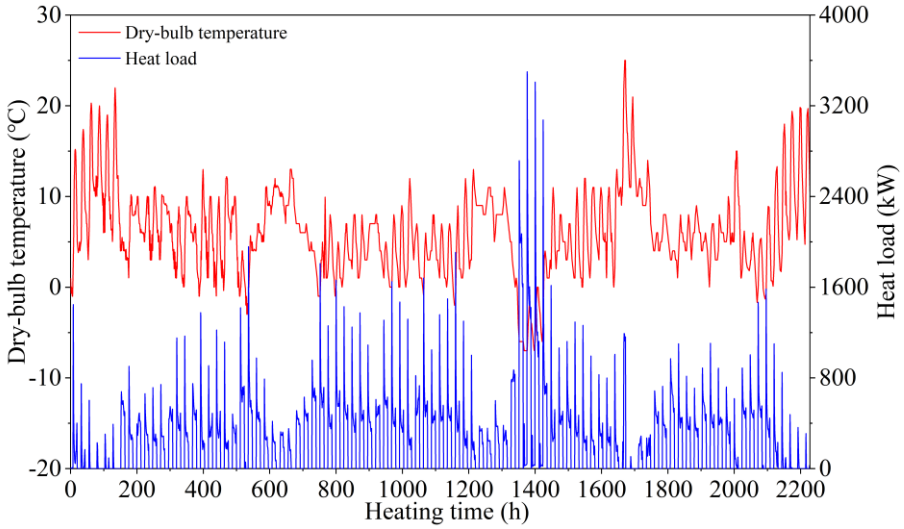

(**c**)

Figure 3. Annual hourly load variations of commercial buildings across different regions: (**a**) Harbin, (**b**) Beijing, (**c**) Shanghai.

3.2. Impact of Outdoor Dry-Bulb Temperature on the Heat Pump Operating Characteristics

The performance of the air-source heat pump systems is significantly influenced by the outdoor meteorological parameters. Focusing on the commercial buildings in Beijing, the impact of outdoor dry-bulb temperatures on the operating characteristics of air-source heat pump systems is investigated in this section. Based on the outdoor temperature data during the heating duration in Beijing, the coldest day (−11.7 °C), the hottest day (0.6 °C), and the moderate-temperature day (a day with average temperature during the heating period, −6.3 °C) were selected for the performance analysis. As shown in Figure 4, the variation trends in the operating units and the system COP of air-source heat pump system on three typical days were simulated.

The results show that the operating unit of heat pump closely follows the variation trend of the building load. As shown in Figure 4a, on the coldest day, to ensure that the indoor temperature in the office buildings does not drop below 5 °C, there is still a low heat load during the non-working hours. However, as shown in Figure 3b, the heat pump system does not need to operate because the thermal storage tank is sufficient to meet the building's heating demand. Additionally, from Figure 4d, f, on the moderate temperature day and the hottest day, there are 1–2 h of temporary shutdown for the heat pump system. This is because the thermal storage tank can meet the heating demand during the durations. Subsequently, as the building load increases, the stored heat in the tank becomes insufficient to meet the demand, causing the heat pump system to restart. During peak load periods on three representative days, the heat pump system needs to operate 39, 17, and 3 units, respectively, to meet the heating demand on the coldest, moderate-temperature, and warmest days. Additionally, the daily average COP of

the heat pump system decreases with the decline in the average temperature of the typical days, being 3.1, 2.8 and 2.5, respectively.

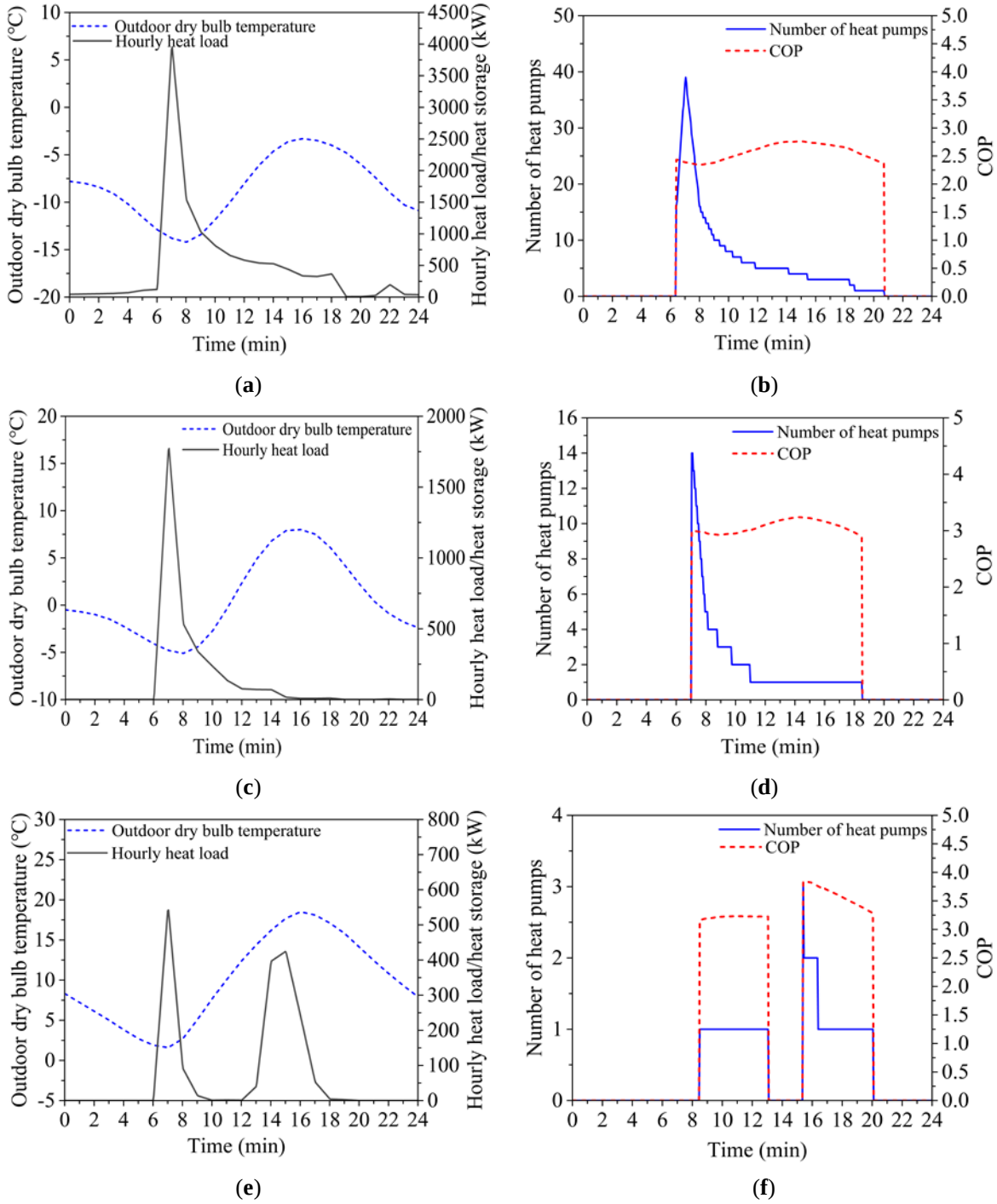

Figure 4. Variation of building load: (**a**) Coldest day; (**c**) Moderate-temperature day; (**e**) Hottest day, and heat pump system operating characteristics: (**b**) Coldest day; (**d**) Moderate-temperature day; (**f**) Hottest day.

3.3. Impact of Climate Zonings on the Heat Pump Operating Characteristics

In the different climate zonings, the setup requirements for air-source heat pump systems vary, including aspects such as supply/return water temperatures, defrosting, and low-temperature corrections, all of which can impact the overall performance of the heat pump system. Therefore, this section will analyze the working characteristics of an air-source heat pump system in the office building under three different climate zonings, with a focus on its performance on the coldest day. As shown in Figure 5, the heat load of office buildings exhibits two peak values, occurring at the beginning and end of the working hours, mainly influenced by the trend of outdoor temperature changes. Additionally, in Harbin, the lower outdoor temperatures at night result in a minimal heat load required to maintain indoor temperatures above 5 °C during non-working hours.

The operating characteristics of the heat pump system vary significantly across the three cities. In Harbin, the heat pump system operates during both working and non-working hours, with up to 15 units running at peak times. During the certain non-working periods, 1–3 units are still required to maintain the heating demand. The hourly fluctuations in the system COP are more pronounced in Harbin compared to Beijing and Shanghai, with a daily average COP of 1.7. In Beijing, due to the smaller heat load, the installation of thermal storage tank allows the heat pump system to operate only during the certain working hours (7 AM to 1 PM), with a maximum of 3 units running. The daily average COP of the heat pump system in Beijing is 2.46, slightly lower than that in Shanghai, which is 2.49.

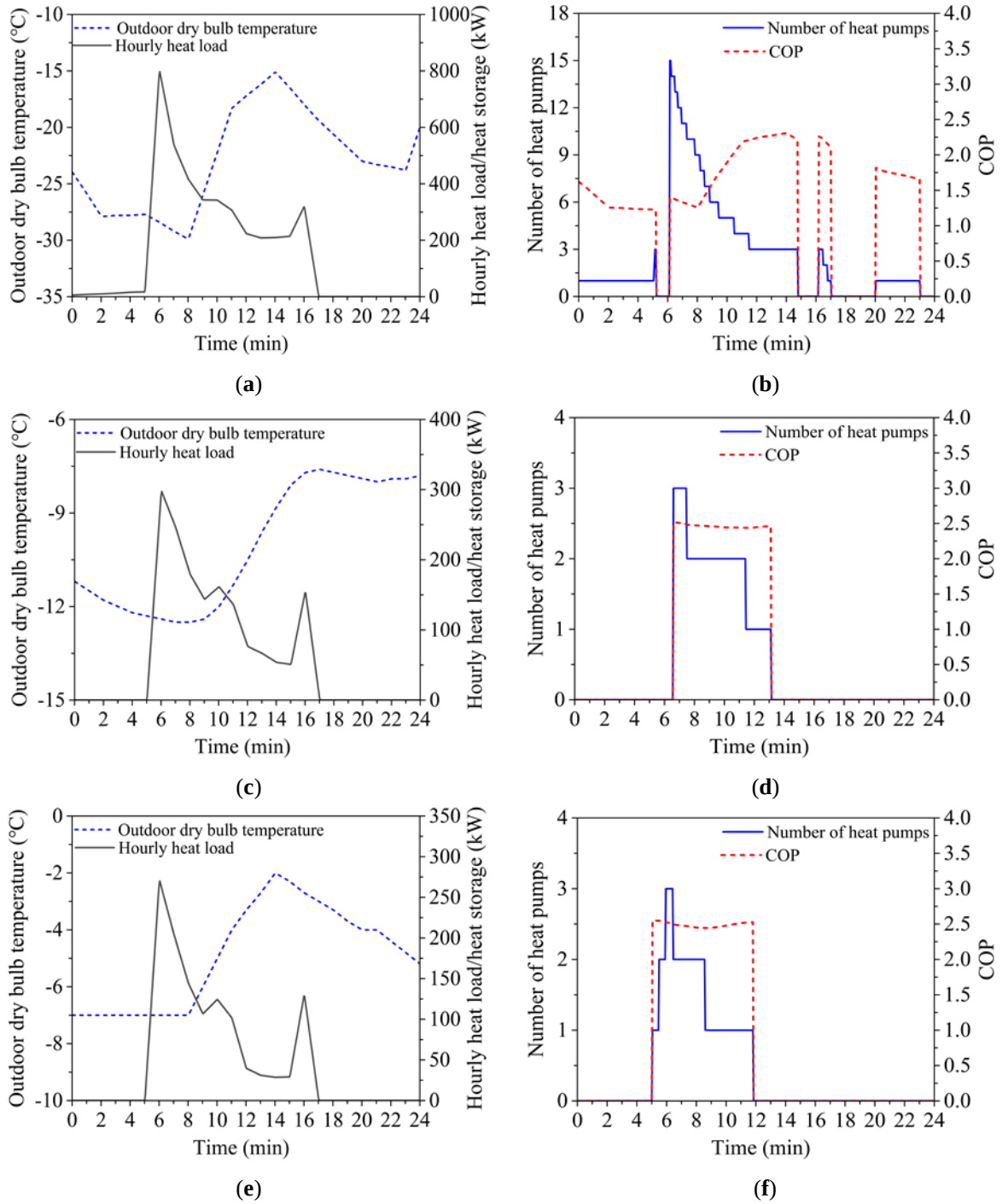

Figure 5. Variation of building load: (**a**) Harbin; (**c**) Beijing; (**e**) Shanghai, and heat pump system operating characteristics: (**b**) Harbin; (**d**) Beijing; (**f**) Shanghai.

3.4. Impact of Public Building Type on the Heat Pump Operating Characteristics

The office, hotel, and commercial buildings differ significantly regarding building area, operating hours, and building load. Focusing on the moderate-temperature day in Shanghai, the impact of public building types on the operating characteristics of air-source heat pump systems is discussed in this section. As descripted in Figure 6, the heat load variation trends of the three types of public buildings show differences in both the load magnitude and heating duration. On moderate-temperature days, the peak load for the office, hotel, and commercial buildings are 70 kW, 1050 kW, and 900 kW, respectively. Additionally, the hotel buildings have the heat load almost 24 hours on moderate-temperature day.

The variation in the operating unit number of heat pump in the hotel building closely aligns with the changes in the building load, with brief periods of shutdown observed. In contrast, with the assistance of the thermal storage tank, only a few heat pumps need to operate in office and commercial buildings during the certain periods to meet the heating demand. The daily average temperatures on the moderate-temperature days are 1.38 °C for the office building, 2.83 °C for the hotel, and 4.07 °C for the commercial building. The daily average COP of the heat pump systems for the office, hotel, and commercial buildings are 2.76, 2.88, and 3.09, respectively. Thus, it can be inferred that the COP of the heat pump systems in different public buildings will exhibit slight differences when the outdoor temperatures are similar.

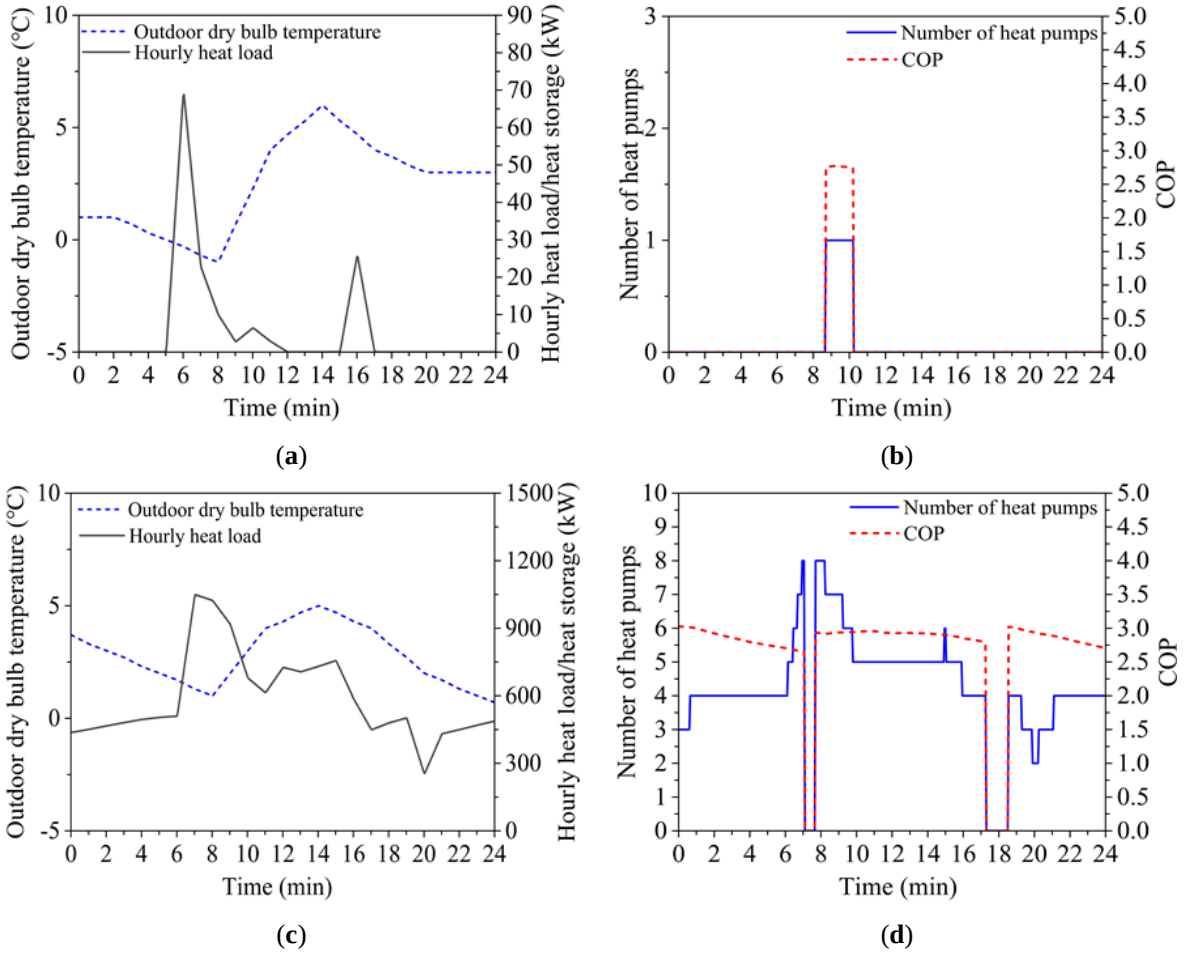

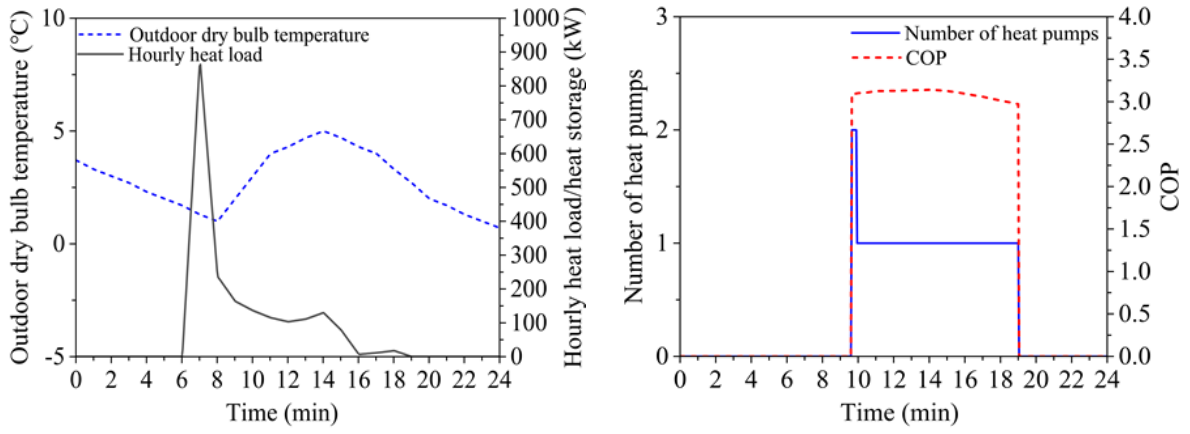

(**e**) (**f**)

Figure 6. Variation of building load: (a) Office; (c) Hotel; (e) Commercial, and heat pump system operating characteristics:(a) Office; (c) Hotel; (e) Commercial.

4. Correlation Analysis of Factors Affecting Heat Pump System Performance

The previous analysis of air-source heat pump heating systems reveals that the dry-bulb temperature significantly affects the system's COP. The building load also affects the system COP, while the building type has a negligible influence on the system COP. To validate the impact of these factors on the system COP, a correlation analysis is required. In this analysis, the dry-bulb temperature, building load, and COP are continuous variables, whereas the public building type is a categorical variable.

For the correlation analysis between the continuous data, Pearson correlation coefficient is used when the data sets of two variables satisfy the normal distribution and show a linear relationship. Spearman correlation coefficient is used when the data sets do not satisfy the normal distribution and linear relationship but show a monotonic relationship. The Pearson and Spearman correlation coefficients are calculated based on Equations (7) and (8), respectively. A one-way analysis of variance (ANOVA) is used to analyze the correlation between continuous data and unordered categorical data.

$$R = \frac{\sum (X - \bar{X})(Y - \bar{Y})}{\sqrt{\sum (X - \bar{X})^2 (Y - \bar{Y})^2}} \tag{7}$$

where R represents the correlation coefficient, and $\bar{X}$ and $\bar{Y}$ are the means of the variables X and Y, respectively.

$$R_S = 1 - \frac{6\sum d^2}{n(n^2 - 1)} \tag{8}$$

where R_S represents the correlation coefficient, d is the difference in ranks between two variables, and n is the sample number.

The Pearson and Spearman correlation coefficients range between −1 and 1, with the values closer to −1 or 1 indicating a stronger correlation. When the coefficient is above 0.5, the variables are positively correlated. When the coefficient is below −0.5, they are negatively correlated. The significance of both correlation coefficients is determined by a p-value below 0.05, indicating a significant correlation between the variables. In one-way ANOVA, the F-value represents the ratio of between-group variance to within-group variance, indicating the extent of the factor influence on the dependent variable. A larger F-value suggests greater significance of differences between groups and smaller significance within groups. A significance level of p-value below 0.05 indicates the significant differences between the different categories of the dependent variable, thereby demonstrating a correlation between the two variables.

The data on the dry bulb temperature, building load, and the COP of air-source heat pump systems for three types of buildings in different regions on the typical days are shown in Table 6. According to the correlation analysis, the Pearson correlation coefficient between the dry-bulb temperature and COP is 0.924, with a p-value of 8.67×10^{-16} below 0.05. The Spearman correlation coefficient is 0.941, with a p-value of 1.59×10^{-17} below 0.05. It indicates that the correlation between the dry-bulb temperature and COP is significant and positively

correlated. The Pearson correlation coefficient between building load and COP is −0.643, with a *p*-value of 0.000024 below 0.05, while the Spearman correlation coefficient is −0.580, with a *p*-value of 0.000207 below 0.05. This indicates that the correlation between building load and COP is significant and negatively correlated. The results of the one-way ANOVA for building types and COP are presented in Table 7. The homogeneity of variance tests all yielded values above 0.05, validating the use of the one-way ANOVA. These results indicate that there is no correlation between building types and COP.

Table 6. The dry-bulb temperature, building load, and system COP on the typical days.

Cities	Typical Day	Building Type	Dry−Bulb Temperature/°C	Heat Load/kW	COP
Harbin	Hottest day	Commercial	7.36	116.48	3.32
		Hotel	10.71	183.31	3.56
		Office	7.91	19.57	3.51
	Coldest day	Commercial	−23.56	1099.65	1.64
		Hotel	−22.99	1832.50	1.78
		Office	−23.54	177.86	1.70
	Moderate−temperature day	Commercial	−8.10	294.42	2.77
		Hotel	−4.13	751.41	3.06
		Office	−3.43	189.12	3.04
Beijing	Hottest day	Commercial	13.22	46.03	3.41
		Hotel	4.81	351.02	3.14
		Office	0.56	163.05	3.12
	Coldest day	Commercial	−7.70	764.18	2.57
		Hotel	−8.52	1084.09	2.61
		Office	−11.65	149.02	2.46
	Moderate−temperature day	Commercial	2.48	208.94	3.07
		Hotel	0.54	669.10	3.06
		Office	−6.30	112.66	2.75
Shanghai	Hottest day	Commercial	10.85	30.37	3.58
		Hotel	10.50	248.02	3.15
		Office	10.37	52.92	3.07
	Coldest day	Commercial	−4.57	235.91	2.81
		Hotel	−4.92	1035.13	2.52
		Office	−5.95	141.84	2.49
	Moderate−temperature day	Commercial	4.07	74.35	3.09
		Hotel	2.83	585.37	2.88
		Office	1.38	4.66	2.76

Table 7. One-way ANOVA of building types and cop.

Cities	Homogeneity of Variance	F-Value	*p*-Value	Correlation
Harbin	0.978 > 0.05	0.043	0.958 > 0.05	NA
Beijing	0.699 > 0.05	0.390	0.679 > 0.05	NA
Shanghai	0.893 > 0.05	0.343	0.712 > 0.05	NA

5. Conclusions

Considered the influence of low temperatures and defrosting conditions, this study established an air-source heat pump heating system model using TRNSYS. The effects of outdoor meteorological parameters, climate zonings, and building types on the operational characteristics and energy efficiency of air-source heat pump systems were simulated and analyzed. By thoroughly comprehending the intricacies of these characteristics and patterns, and integrating them with the actual demands of buildings for intelligent adjustments, the heat pump systems can achieve substantial improvements in energy efficiency, ensuring a comfortable indoor environment simultaneously. The key conclusions of this study are as follows.

1. In terms of the annual load variation, the building heat load in Harbin and Beijing reach the peak in the middle of the heating season, whereas that in Shanghai shows a more moderate variation in annual building load. The variations in the operation unit number of heat pump system closely mirror the variation in the building load.

2. The performance of air-source heat pumps is closely tied to climate zonings. On the coldest day of the heating duration, the daily average COP of air-source heat pump heating systems in Harbin, Beijing, and Shanghai was as follows: Shanghai (2.49) > Beijing (2.46) > Harbin (1.7).

3. Through the combination of correlation coefficients and one-way ANOVA, it was found that the COP of air-source heat pump heating systems is positively correlated with dry bulb temperature and negatively correlated with the building load, independent of the building type in the public buildings.

Author Contributions: J.F.: software, data curation, writing-original draft preparation; Y.L.: conceptualization, methodology, writing-reviewing and editing; J.M.: visualization, investigation; Y.C.: data curation, supervision; Z.Z.: software, validation; X.C.: validation, supervision; L.J.: supervision, writing-reviewing and editing. All authors have read and agreed to the published version of the manuscript.

Funding: This research was funded by National Natural Science Foundation of China, 52406109, Fundamental Research Funds for the Central Universities, xzy012024075, Shaanxi Postdoctoral Science Foundation, 2023BSHEDZZ51 and Postdoctoral Fellowship Program of CPSF, GZC20232076.

Institutional Review Board Statement: Not applicable.

Informed Consent Statement: Written informed consent has been obtained from the patients to publish this paper.

Data Availability Statement: Not applicable.

Conflicts of Interest: The authors declare no conflict of interest.

Reference

1. Shan, Y.; Guan, D.; Zheng, H.; et al. China CO_2 emission accounts 1997–2015. *Sci. Data* **2018**, *5*, 170201.
2. Du, W.; Li, X.; Chen, Y.; Shen, G. Household air pollution and personal exposure to air pollutants in rural China—A review. *Environ. Pollut.* **2018**, *237*, 625–638.
3. Cai, J.Y.; Zhou, H.H.; Xu, L.J.; et al. Experimental and numerical investigation on the heating performance of a novel multi-functional heat pump system with solar-air composite heat source. *Sustain. Cities Soc*. **2021**, *73*, 103118.
4. Ni, L.; Dong, J.; Yao, Y.; et al. A review of heat pump systems for heating and cooling of buildings in China in the last decade. *Renew. Energy* **2015**, *84*, 30–45.
5. Vieira, A.S.; Stewart, R.A.; Beal, C.D. Air source heat pump water heaters in residential buildings in Australia: Identification of key performance parameters. *Energy Build.* **2015**, *91*, 148–162.
6. Wei, W.Z.; Wu, C.S.; Ni, L.; et al. Performance optimization of space heating using variable water flow air source heat pumps as heating source: Adopting new control methods for water pumps. *Energy Build.* **2022**, *255, 111654*.
7. Zhang, Q.; Zhang, L.; Nie, J. Techno-economic analysis of air source heat pump applied for space heating in northern China. *Appl. Energy* **2017**, *207*, 533–542.
8. Zhang, L.; Jiang, Y.; Dong, J. Advances in vapor compression air source heat pump system in cold regions: A review. *Renew. Sustain. Energy Rev*. **2018**, *81*, 353–365.
9. Safa, A.A.; Fung, A.S.; Kumar, R. Comparative thermal performances of a ground source heat pump and a variable capacity air source heat pump systems for sustainable houses. *Appl. Therm. Energy* **2015**, *81*, 279–287.
10. Zhang, H.; Jiang, L.; Zheng, W.; et al. Experimental study on a novel thermal storage refrigerant-heated radiator coupled with air source heat pump heating system. *Build. Environ.* **2019**, *164*, 106341.
11. Xu, X.; Fang, Z.; Wang, Z. Climatic division based on frosting characteristics of air-source heat pumps. *Energy Build.* **2020**, *224*, 110219.
12. Wu, C.; Liu, F.; Li, X.; et al. Low-temperature air source heat pump system for heating in severely cold area: Long-term applicability evaluation. *Build. Environ.* **2022**, *208*, 108594.
13. Wu, P.; Wang, Z.; Li, X.; et al. Energy-saving analysis of air source heat pump integrated with a water storage tank for heating applications. *Build. Environ.* **2020**, *180*, 107029.
14. Long, J.; Xia, K.; Zhong, H.; et al. Study on energy-saving operation of a combined heating system of solar hot water and air source heat pump. *Energy Convers. Manag.* **2021**, *229*, 113624.
15. Song, M.; Deng, S.; Dang, C. Review on improvement for air source heat pump units during frosting and defrosting. *Appl. Energy* **2018**, *211*, 1150–1170.
16. Wang, X.; Yu, J.; Xing, M. Performance analysis of a new ejector enhanced vapor injection heat pump cycle. *Energy Convers. Manag.* **2015**, *100*, 242–248.
17. Wei, W.; Ni, L.; Zhou, C. Performance analysis of a quasi-two stage compression air source heat pump in severe cold region with a new control strategy. *Appl. Therm. Eng*. **2020**, *174*, 115317.
18. Li, Y.; Yu, J. Theoretical analysis on optimal configurations of heat exchanger and compressor in a two-stage compression air source heat pump system. *Appl. Therm. Eng.* **2016**, *96*, 682–689.
19. Soltani, R.; Dincer, I.; Rosen, M.A. Comparative performance evaluation of cascaded air-source hydronic

heat pumps. *Energy Convers. Manag.* **2015**, *89*, 577–587.
20. Shen, J.; Guo, T.; Tian, Y. Design and experimental study of an air source heat pump for drying with dual modes of single stage and cascade cycle. *Appl. Therm. Eng.* **2018**, *129*, 280–289.
21. Karami, M.; Abdshahi, H. Energy and exergy analysis of the transient performance of a qanat-source heat pump using TRNSYS-MATLAB co-simulator. *Energy Environ.* **2023**, *34*, 560–585.
22. Loïc, C.; Rowley, P. Towards low carbon homes—A simulation analysis of building-integrated air-source heat pump systems. *Energy Build.* **2012**, *34*, 127–136.